SUPPLEMENTARY MATERIAL

Potential Signatures and the Means of Detecting a Hypothetical Ground Source Cooled Nuclear Reactor

Lance K. Kim, Rainer Jungwirth, Guido Renda, Erik Wolfart, and Giacomo G. M. Cojazzi

SCIENCE & GLOBAL SECURITY
2016, Volume 24, No. 2, pp. 92-113

http://dx.doi.org/10.1080/08929882.2016.1184529

Appendix A: Estimate of Extraction Well Drawdown and Pumping Power

Theis's equation describes the time evolution of the cone of depression around a well pumping from a confined aquifer. The drawdown, s, (the difference in piezometric head, h, from an initial head, H) at a radial distance, r, for a well pumping at a rate, $\dot{V}$, for a period of time, t, drawing upon a confined aquifer with hydraulic conductivity, K, thickness, b, and storativity, S, is,

$$s(r,t) = H - h(r,t) = \left(\dot{V}/(4\pi Kb)\right)\ W[(Sr^2)/(4Kbt)] \qquad \textbf{Equation 1}$$

where the well function, W(u), or exponential integral, E_1,(u), is given by,[1]

$$W(u) = E_1(u) = \int_u^{\infty} \exp(-x)/x\ dx \qquad \textbf{Equation 2}$$

The storativity of a confined aquifer is the product of the specific storage, S_S, and the thickness of the confined aquifer,

$$S = bS_S = b[\rho g(\beta_r + \varphi\beta_w)] \qquad \textbf{Equation 3}$$

where the specific storage is related to the fluid density, ρ, gravitational acceleration, g, porosity, ϕ, compressibility of the aquifer material, β_r (assumed equivalent to jointed rock), and compressibility of water, β_w.[2]

Table 1 Estimate of aquifer storativity

Property	Value	
Aquifer Thickness, b (m)	50	
Fluid Density, ρ (kg/m^3)	1000	
Porosity, ϕ	0.14	
Compressibility, Water, β_w, (Pa^{-1})	$4.4X10^{-10}$	
Compressibility, Jointed Rock, β_r, (Pa^{-1})	10^{-10}	10^{-8}
Specific Storage, S_S	$2X10^{-6}$	$1X10^{-4}$
Storativity, S	$8X10^{-5}$	$5X10^{-3}$

The time evolution of the cone of depression is shown in Figure 1 for a 8900m^3/s well sufficient for a 30MWt reactor drawing upon a 50m thick confined aquifer with a storativity of $5X10^{-3}$. The

evolution of drawdown at the well casing over time is displayed in Figure 2 which also shows the effects of an two order of magnitude reduction in storativity. As indicated in these figures, geologic media with higher permeability and compressibility lead to shallower drawdowns. Note that these results are inapplicable should unconfined pumping conditions arise when the drawdown drops below the aquifer's top confining layer.

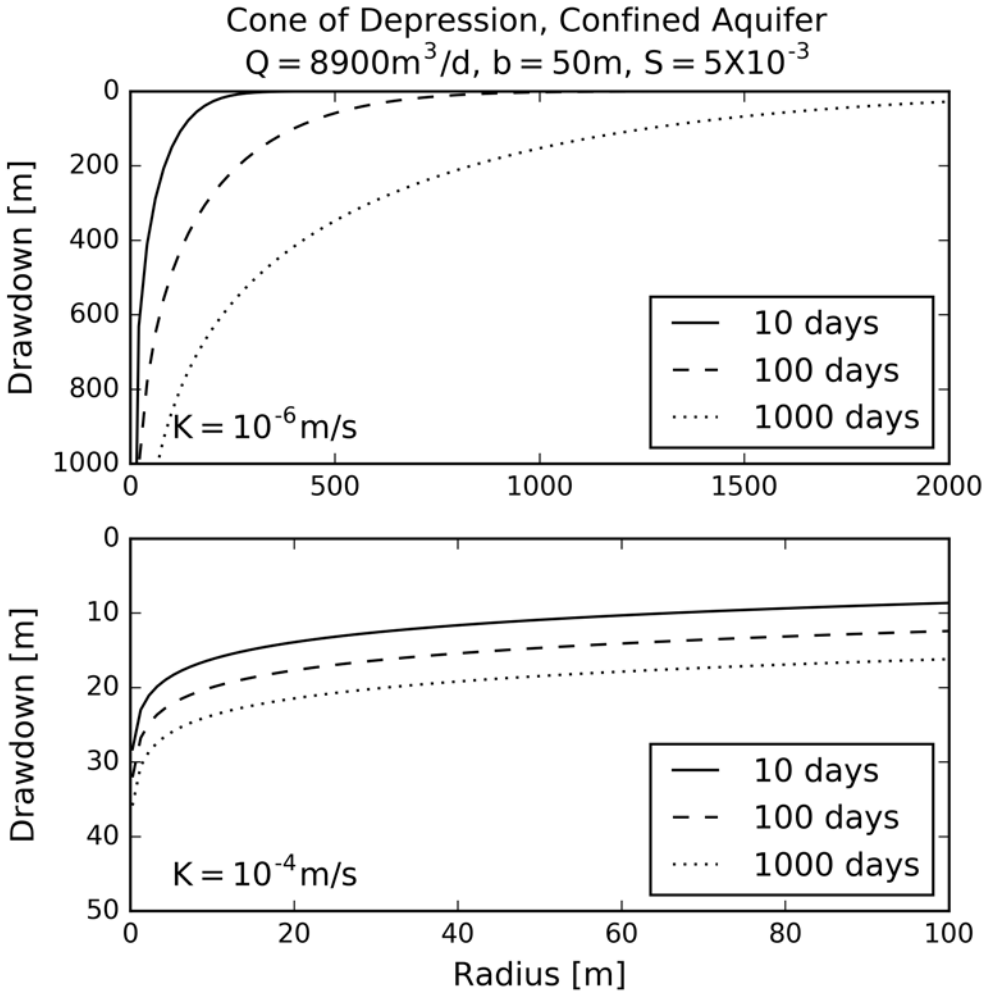

Figure 1. Cone of depression at selected times for a 8900m^3/s well extracting from a 50m thick confined aquifer with a storativity of 5X10^{-3}

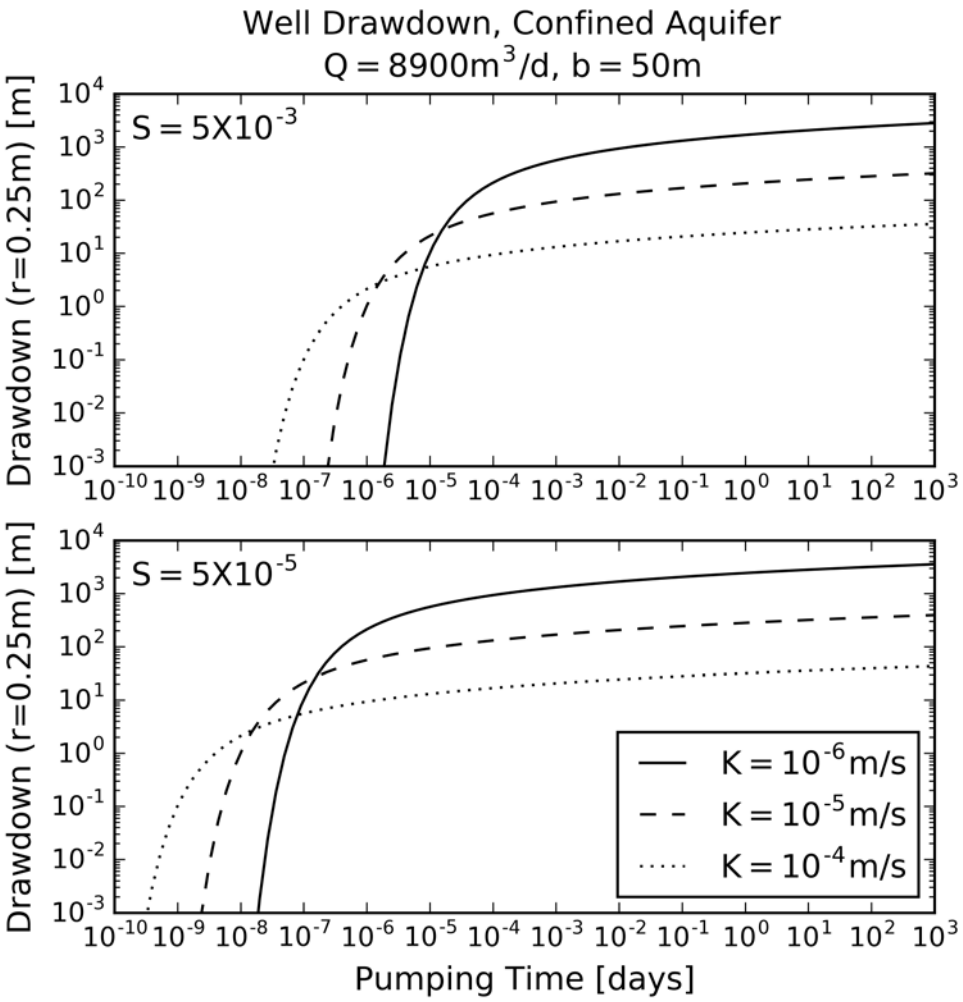

Figure 2. Time evolution of drawdown at the well casing for a 8900m³/s well extracting from a 50m thick confined aquifer with a storativity of 5X10^{-3} (top) and 5X10^{-5} (bottom)

Deeper drawdowns increase pumping power requirements to lift water up the well casing. Well pumps are sized to supply sufficient total dynamic head at the required rate of flow where the total dynamic head is the sum of the head losses up the well casing (well drawdown and additional vertical rise) and friction losses through piping.[3] Ignoring additional vertical rise and friction losses, the mechanical pumping power required to overcome the well drawdown, s, is,

$$P = \rho \dot{V} g s \qquad \textbf{Equation 4}$$

where ρ is fluid density, $\dot{V}$ is pumping rate, g is gravitational acceleration, and s is drawdown at the well casing. The mechanical pumping power is approximately 1kW to overcome every 1m of drawdown at an extraction rate of 8900m^3/day for water with a density of 1000kg/m^3. An equivalent amount of pumping power is required for the vertical rise above the static water level in addition to the power required to overcome frictional losses through piping.

APPENDIX B: GEOTHERMAL POWER ANALOGUE

Geothermal power plants are a close analogue to a ground source cooled reactor. There are essentially three types of geothermal energy recovery systems: hot-water (e.g., Dixie Valley, United States), vapor-dominated (e.g., Larderello, Italy), and binary.[4] These systems extract geothermal fluids via production wells to drive a turbine-generator. At many geothermal power plants, cooled geothermal fluids are injected back into the subsurface to dispose of wastewater and to maintain reservoir pressures to prevent subsidence and enhance energy recovery.[5] The operational regime of these injection wells is comparable to those that might be used for a ground source cooled reactor. Injection flow rates vary widely, depending upon the type of plant and geothermal source characteristics.[6] For example, a 30MWe geothermal power plant might inject 150-600kg/s of wastewater at 100-200^{O}C.[7]

A key difference is that the subsurface is a heat source for geothermal power production while it is a heat sink for a ground source cooled reactor. Unlike a nuclear system drawing upon a cold groundwater, a geothermal power plant continues to rely on conventional cooling methods for its ultimate heat sink. Both systems contend with thermal breakthrough.[8] Breakthrough has been observed at geothermal sites and has been largely addressed by relocating injection wells – though breakthrough can have positive effects at geothermal sites by reducing drawdown around extraction wells.[9]

APPENDIX C: EMERGENCY CORE COOLING

Should the extraction well fail to provide adequate cooling water flow, a backup cooling system is desirable to protect the investment from core damage, prevent the release of radionuclides that might be detected via a network of air sampling stations, and protect public health and safety. Following a reactor trip triggered by loss of cooling flow, reactor power quickly drops to approximately 6 percent of the initial power and decays roughly exponentially over time. An air-cooled heat exchanger with a peak cooling capacity of approximately 2MWt (6 percent of 30MWt) is one possibility and could produce thermal signatures. A decay heat boil-off tank is another possibility where gas circulators or water pumps transfer decay heat from the core.[10] Eventually, additional water is required to make-up for evaporative losses from the boil-off tanks – either by restoring flow from the well, reversing flow from an injection well, or acquiring water from off-site.[11]

The size of the decay heat boil-off tank is estimated based on the decay heat energy released over time. Accounting solely for the heat of vaporization of water (Δh_{vap}=2.3MJ/kg), the cumulative amount of water boiled away after shutdown, m(t), is related to the decay heat energy (the integral of the decay heat power, P(t), for a reactor with a thermal power of P_0 in MWt operated for a period of t_o), as follows,[12]

$$
\begin{aligned}
m(t) &= \left(1/\Delta h_{vap}\right) \int_{\tau=0}^{t} P(\tau)d\tau \\
&= \left(1/\Delta h_{vap}\right) \int_{\tau=0}^{t} \left(0.066P_0(\tau^{-0.2} - (\tau + t_0)^{-0.2})\right)d\tau \\
&= \left(1/\Delta h_{vap}\right)\left(0.0825P_0(t^{0.8} - (t + t_0)^{0.8} + t_0^{0.8})\right), \\
&\qquad 10s < t < 100days
\end{aligned}
\qquad \textbf{Equation 5}
$$

As shown in Figure 3 using **Equation 5**, approximately 30m^3 of water boils away after one week, indicating that a modestly sized decay heat boil-off tank holds sufficient water to cool the reactor before requiring make-up.

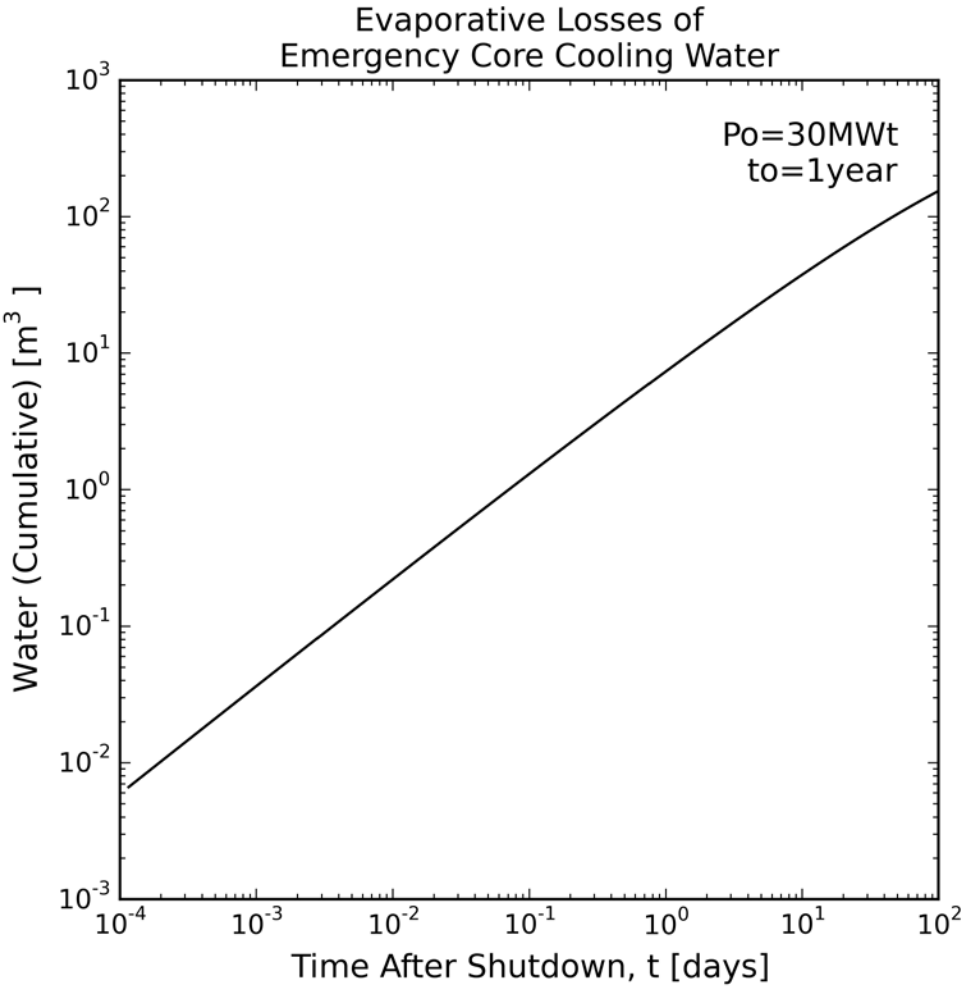

Figure 3. Estimated evaporative losses of cooling water following shutdown of a 30MWt reactor after one year of operation

APPENDIX D: ESTIMATED AREAL EXTENT OF THE THERMAL PLUME

Heat transfer from the underground thermal plume to the ground surface may present the largest temperature affected area visible to satellite-borne thermal infrared imaging. The temperature affected area of the aquifer characterized by porous flow is estimated in the absence of a regional groundwater flow using the ratio between the injected volume of the aquifer from which groundwater has been displaced, V_A, and the volume of the aquifer where the temperature has been altered, V_T. This ratio is given as follows and is related to the porosity of the rock, ϕ, density, ρ, and specific heat, C, of the rock, R, and water, W, [13]

$$(V_A/V_T) = \left((1-\phi)\rho_R C_R + \phi\rho_W C_W\right)/(\phi\rho_W C_W) \qquad \textbf{Equation 6}$$

The volume of the aquifer from which groundwater is displaced is related to the volume of water, V_w, and porosity of the aquifer matrix, ϕ,

$$V_A = V_W/\phi \qquad \textbf{Equation 7}$$

Assuming that a reactor produces 1g of plutonium per MWD of thermal energy, a 30MWt reactor produces a significant quantity (8 kg) of plutonium after 270 days and discharges approximately $2.4\text{x}10^6$ m^3 of cooling water.[14] Assuming porous flow from a cylindrical injection well intercepting a 50m thick limestone aquifer (ρ_R=2500kg/m^3, c_R=0.85 kJ/kg K, φ=0.14, Table 2 [15]), the areal extent of the displaced water zone is equivalent to a cylinder approximately 660m in diameter (**Equation 7**) and the temperature affected zone is approximately 330m in diameter (**Equation 6**).

Table 2: Properties of limestone

Property	Value
Density, ρ_R (kg/m^3)	2410 – 2690
Thermal Conductivity, k_g (W/mK)	2.3 – 3.44
Heat Capacity, C_R (kJ/kg K)	0.844 – 0.851
Hydraulic Conductivity, K (m/s)	$1\text{x}10^{-6}$ – $1\text{x}10^{-2}$
Effective Porosity, ϕ	~0-0.36 (mean: 0.14)

APPENDIX E: ESTIMATE OF PEAK GROUND SURFACE TEMPERATURE

To detect a buried heat source via satellite-borne thermal infrared imagery, the ground surface temperature must have an effective temperature averaged over an imager pixel's field of view greater than the temperature threshold.[16] The depth of burial to minimize surface thermal anomalies from blind low-enthalpy sources depends upon the complex effects of the surface energy balance composed of radiative, sensible, latent, and ground heat fluxes, energy storage in interfacial layers (e.g. vegetation, buildings), and the effects of soil moisture on the thermophysical properties of the ground.[17]

Ground surface temperature depends on a complex time-dependent heat balance that follows diurnal and annual patterns. The net radiative energy, R_N, incident upon the surface is distributed between sensible, H_S, latent, H_L, and ground, H_G, heat fluxes; and the energy stored in interfacial layers per unit area, W(t),

$$R_N = H_S + H_L + H_G + dW/dt \qquad \textbf{Equation 8}$$

External radiation forcing, R_N, is composed of the net shortwave solar radiation incident on the surface and net longwave thermal radiation between the ground and sky. This energy is distributed between convective and conductive heat transfer from the ground to the air (sensible heat flux, H_S), heat loss from the ground and vegetation to the air due to the evaporation of moisture (latent heat flux, H_L), heat conduction into the ground (ground heat flux, H_G), and energy storage in vegetation and buildings (W(t)).[18]

The relative contribution of these various heat transfer mechanisms varies by location, ground properties, and exhibits diurnal and annual patterns. For example, solar radiation from the rising sun warms the ground that then heats the surrounding air, promoting convective cooling of the surface and evaporative cooling of the ground. At night, absent a cooling breeze and other significant heat transfer mechanisms, the heated ground is predominantly cooled by thermal radiation to the night sky.

(Figure 4) In response to these heating and cooling patterns, the profile of ground temperature with depth follows a diurnal and annual cycle where the amplitude of the temperature "wave" penetrating the subsurface attenuates with depth and lags the surface temperature in time.[19]

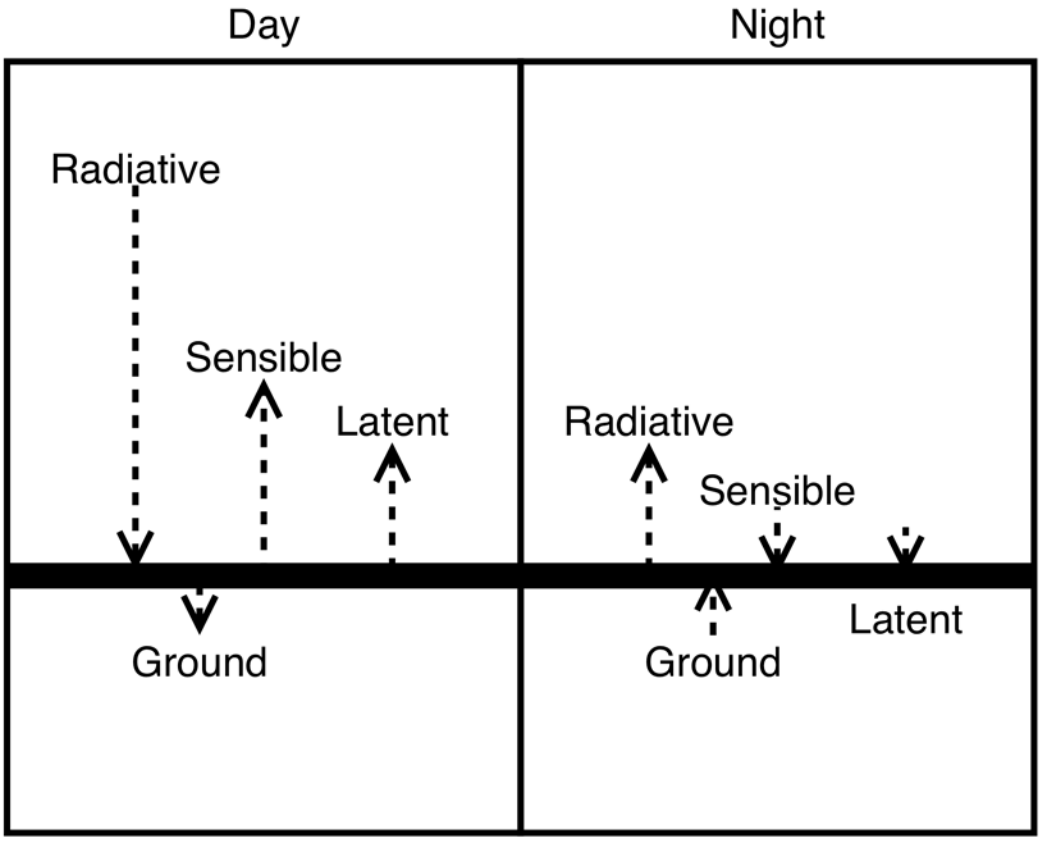

Figure 4. Example of daytime and nighttime heat fluxesA simplified estimate of the peak steady state ground surface temperature is obtained by approximating the buried hot leg, injection well, and thermal plume as a constant temperature planar heat source buried below the ground surface. On a calm cloudless night, radiation heat transfer to the sky is assumed to be the dominant heat transfer mechanism from the ground surface as a satellite passes overhead. (Figure 5) This assumption is valid for dry, bare ground under calm conditions where radiative heat losses dominate sensible and latent heat transfer.[20] Though highly idealized, this model approximates the nighttime ground temperature directly above these heat sources where the temperature is highest.

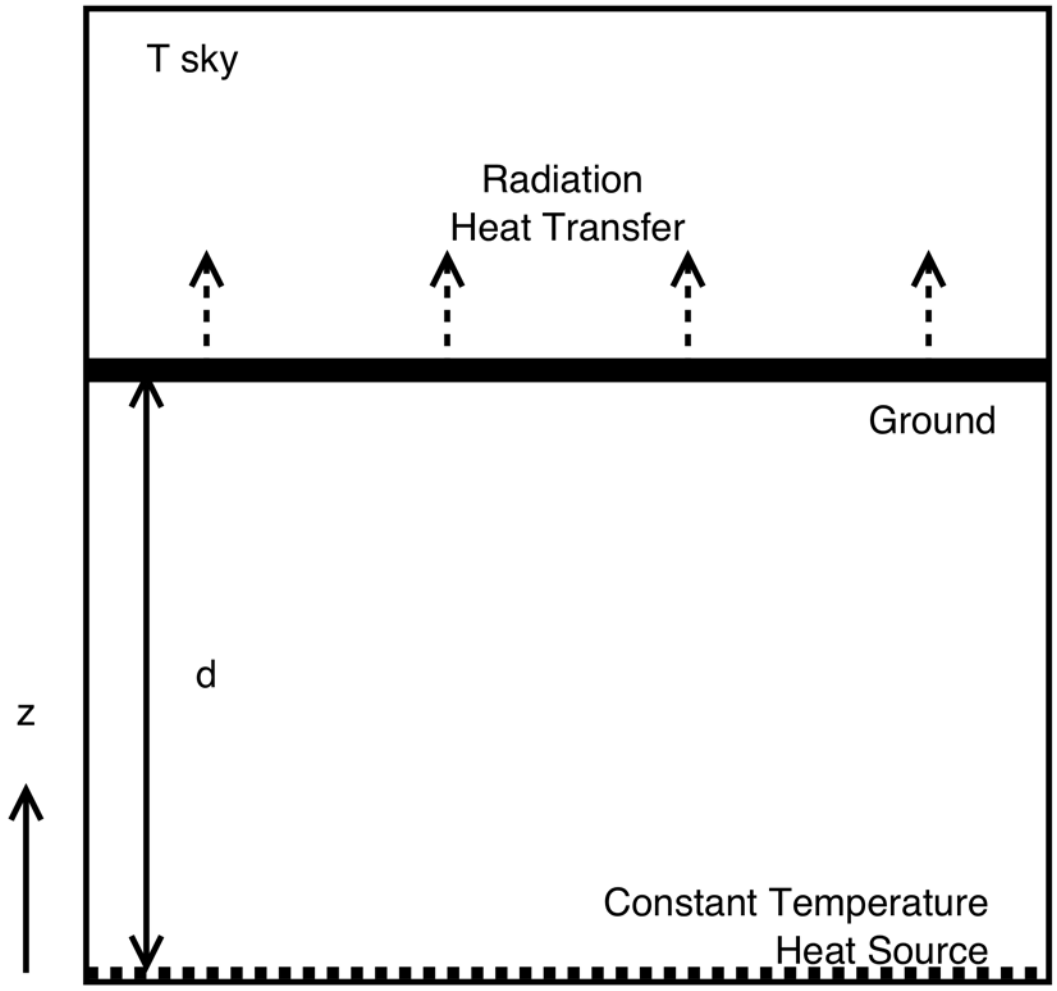

Figure 5. Schematic of the model to estimate ground surface temperature cooled by radiation heat transfer to the sky and heated by a buried constant temperature heat source

In one dimension without internal heat generation, the steady-state heat diffusion equation simplifies to,

$$d^2T/dz^2 = 0 \qquad \textbf{Equation 9}$$

The buried pipeline, injection well, and thermal plume is approximated as a constant temperature boundary condition,

$$T|_{z=0} = T_{hot} \qquad \textbf{Equation 10}$$

The heated ground surface is assumed to be cooled by radiative heat transfer to the night sky and modeled as a small gray body of emissivity, ε, radiating to the much larger sky at an effective temperature, T_{sky}, as follows,

$$-k_g(dT/dz)\big|_{z=d} = \varepsilon\sigma\left(T^4 - T_{sky}^4\right)\big|_{z=d} \qquad \textbf{Equation 11}$$

where T is the ground temperature as a function of depth, k_g is the thermal conductivity of the ground, d is depth of burial, and σ is the Stefan-Boltzmann constant.

In the absence of cloud cover, the effective temperature of the sky is related to the dew-point temperature, T_{dp}, reflecting the air temperature, humidity, and the time of day by,

$$T_{sky} = T_{air}\left[0.711 + 0.0056T_{dp} + 7.3 \times 10^{-5}T_{dp}^2 + 0.013\cos(2\pi t/24)\right]^{0.25}, -20^0C < T_{dp} < 30^0C \qquad \textbf{Equation 12}$$

where T_{sky} and T_{air} are in Kelvin, T_{dp} is in ^{O}C, and t is the hour past midnight.[21]

Solving the heat diffusion equation (**Equation 9**) under these boundary conditions (**Equation 10**, **Equation 11**), the vertical ground temperature profile for a burial depth, d, is given by,

$$T(d) = T_{hot} - \left(d\varepsilon\sigma/k_g\right)\left(T(d)^4 - T_{sky}^4\right) \qquad \textbf{Equation 13}$$

Assuming that the desired ground surface temperature, T(d), is no more than 0.2^{O}C above the ambient air temperature, T_{air}, to avoid detection (i.e. the temperature of undisturbed ground temperature is assumed equal to air temperature), the necessary depth of burial is solved iteratively using **Equation 13**. For limestone, the necessary burial depth is on the order of 4m for the values of thermal conductivity, emissivity, air temperature, and humidity shown in Table 3. Exploiting the temperature averaging of the imager, reducing injection temperature, or emplacing insulating material around the pipeline and well reduces burial depth. Given the simplifications and assumptions, these results should

only be considered as an "order of magnitude" estimate of burial depth – a more realistic estimate would account for other heat transfer mechanisms (e.g., sensible, latent, and ground heat fluxes) and daytime insolation that affects the evolution of the ground temperature profile.

Table 3: Estimated depth of burial to limit peak ground temperature below the detection threshold of thermal infrared imagery

Parameter	Value					
Hot Temperature, T_{hot} (°C)	90					
Ground Thermal Conductivity, k_g (W/mK)	3.4					
Detection Threshold (°C)	0.2					
Relative Humidity (percent)	50					
Air Temperature, T_{air} (°C)	0		10		20	
Ground Surface Temperature (°C)	0.2		10.2		20.2	
Dew-Point Temperature, T_{dp} (°C)	-9.2		0.5		9.3	
Effective Sky Temperature at Midnight, T_{sky} (°C)	-25		-12		3	
Ground Emissivity, ε	0.83	0.95	0.83	0.95	0.83	0.95
Radiation Heat Loss (W/m²)	85	97	85	97	75	86
Burial Depth, d (m)	3.6	3.2	3.2	2.8	3.2	2.8

A study accounting for the complexities of the surface energy balance found that shallow groundwater under flat bare ground is detectable by satellite-borne thermal infrared imagery when the potential for evaporative heat losses are high and/or differences between daytime and nighttime air temperature are sufficiently large. The study showed seemingly counterintuitive results from the complex interaction of soil moisture on the thermophysical properties of the ground and the surface energy balance – deeper groundwater raised daytime ground temperature while lowering nighttime ground temperature, shallow groundwater raised ground temperature in wintertime and lowered ground temperature in summertime, summertime ground temperature effects were more detectable than in wintertime, etc. Below a critical depth, however, ambient groundwater no longer affected surface temperature, surface soil moisture, and the surface energy balance. Under the studied conditions, this critical depth occurs at approximately 1m for well-drained sandy soil with high hydraulic conductivity and low capillarity, and extending to several meters in clayey soil.[22] Unusually warm groundwater

presumably increases critical depth due from heat conduction to the surface, but the necessary analysis considering site-specific conditions is beyond the scope of this paper.

Notes and references

[1] Ekkehard Holzbecher, *Environmental Modeling: Using MATLAB*, 2nd ed. (Springer Berlin Heidelberg, 2012).

[2] Glenn M. Duffield, "Representative Values of Hydraulic Properties," *AQTESOLV*, 2015, http://www.aqtesolv.com/aquifer-tests/aquifer_properties.htm.

[3] National Exploration, Wells and Pumps, "Submersible Pump Sizing and Selection," n.d., https://www.ihs.gov/EHSCT/documents/sfc_webinar_docs/2013-Pump%20Sizing%20With%20Exercises%20r1.pdf.

[4] U.S. Geological Survey, Wendell A. Duffield, and John H. Sass, "Geothermal Energy - Clean Power From the Earth's Heat," 2003, http://pubs.usgs.gov/circ/2004/c1249/c1249.pdf; "Visita Alle Centrali," *Enel*, 2009, http://servizi.enel.it/visitacentrali/it/geotermica/geotermica.asp.

[5] Gudmundur S. Bodvarsson and Valgardur Stefansson, "Some Theoretical and Field Aspects of Reinjection in Geothermal Reservoirs," *Water Resources Research* 25, no. 6 (1989): 1235–48.

[6] Eylem Kaya, Sadiq J. Zarrouk, and Michael J. O'Sullivan, "Reinjection in Geothermal Fields: A Review of Worldwide Experience," *Renewable and Sustainable Energy Reviews* 15, no. 1 (2011): 47–68.

[7] G. Bodvarsson, "Thermal Problems in the Siting of Reinjection Wells," *Geothermics* 1, no. 2 (1972): 63–66.

[8] Gudmundur S. Bodvarsson and Valgardur Stefansson, "Reinjection into Geothermal Reservoirs," in *Geothermal Reservoir Engineering*, ed. Ender Okandan, vol. 150, NATO ASI Series (Springer Netherlands, 1988).

[9] Kaya, Zarrouk, and O'Sullivan, "Reinjection in Geothermal Fields: A Review of Worldwide Experience."

[10] International Atomic Energy Agency, "General Design and Principles of the Advanced Gas-Cooled Reactor (AGR)," *IAEA International Knowledge Base on Nuclear Graphite*, 2015, http://nucleus.iaea.org/sites/graphiteknowledgebase/wiki/Guide_to_Graphite/General%20Design%20and%20Principles%20of%20the%20Advanced%20Gas-Cooled%20Reactor%20(AGR).aspx.

[11] Kaya, Zarrouk, and O'Sullivan, "Reinjection in Geothermal Fields: A Review of Worldwide Experience."

[12] Neil E. Todreas and Mujid S. Kazimi, *Nuclear Systems I, Thermal Hydraulic Fundamentals* (Hemisphere Publishing Corporation, 1990).

[13] Marcelo J. Lippmann and Chin Fu Tsang, "Ground-Water Use for Cooling: Associated Aquifer Temperature Changes," *Ground Water* 18, no. 5 (October 1980); Walter J. Schaetzle et al., *Thermal Energy Storage in Aquifers: Design and Applications* (Pergamon Press, 1980).

[14] "Plutonium Production," *Federation of American Scientists*, June 20, 2000, http://www.fas.org/nuke/intro/nuke/plutonium.htm; International Atomic Energy Agency, "IAEA Safeguards Glossary," International Nuclear Verification Series (Austria, 2002), http://www-ns.iaea.org/standards/concepts-terms.asp.

[15] Lev Eppelbaum, Izzy Kutasov, and Arkady Pilchin, *Applied Geothermics*, Lecture Notes in Earth System Sciences (Springer-Verlag Berlin Heidelberg, 2014); C. Yu et al., "Data Collection Handbook to Support Modeling Impacts of

Radioactive Material in Soil" (Argonne National Laboratory, April 1993); National Research Council., *Contaminants in the Subsurface: Source Zone Assessment and Remediation* (Washington, DC: The National Academies Press, 2004).

[16] Hui Zhang and Frank von Hippel, "Using Commercial Imaging Satellites to Detect the Operation of Plutonium Production Reactors and Gaseous-Diffusion Plants," *Science & Global Security* 8 (2000): 219–71; Hui Zhang, "Uses of Commercial Satellite Imagery in FMCT Verification," *The Nonproliferation Review*, Summer 2000.

[17] Orlando B. Andersland and Branko Ladanyi, *An Introduction to Frozen Ground Engineering* (Springer-Verlag US, 1994); Junsei Kondo and Shigenori Haginoya, "Characteristic Heat Transfer Coefficients Near the Ground at Night During Strong Winds," *Boundary-Layer Meteorology* 46, no. 1–2 (1989): 169–80; P. Groen, "Note on the Theory of Nocturnal Radiational Cooling of the Earth's Surface," *Journal of Meteorology* 4, no. 2 (April 1, 1947): 63–66; Kshudiram Saha, "Heat Balance of the Earth's Surface – Upward and Downward Transfer of Heat," in *The Earth's Atmosphere* (Springer Berlin Heidelberg, 2008), 115–36; S. Pal Arya, *Introduction to Micrometeorology*, Second Edition, vol. 79, International Geophysics Series (Academic Press, 2001); F. Alkhaier, R. J. Schotting, and Z. Su, "A Qualitative Description of Shallow Groundwater Effect on Surface Temperature of Bare Soil," *Hydrology and Earth System Sciences* 13 (September 2009): 1749–56; F. Alkhaier, G. N. Flerchinger, and Z. Su, "The Thermodynamic Effect of Shallow Groundwater on Temperature and Energy Balance at Bare Land Surface, Heat Analysis and Thermodynamic Effects," in *Heat Analysis and Thermodynamic Effects*, ed. Amimul Ahsan (Intech, 2011), http://www.intechopen.com/books/heat-analysis-and-thermodynamic-effects; F. Alkhaier, G. N. Flerchinger, and Z. Su, "Shallow Groundwater Effect on Land Surface Temperature and Surface Energy Balance Under Bare Soil Conditions: Modeling and Description," *Hydrology and Earth System Sciences* 16, no. 7 (2012): 1817–31; F. Alkhaier, Z. Su, and G. N. Flerchinger, "Reconnoitering the Effect of Shallow Groundwater on Land Surface Temperature and Surface Energy Balance Using MODIS and SEBS," *Hydrology and Earth System Sciences* 16, no. 7 (2012): 1833–44; F. Alkhaier, "Shallow Groundwater Effect on Land Surface Temperature and Surface Energy Balance: Description, Modeling and Remote Sensing Application" (Doctoral Dissertation, University of Twente, 2011).

[18] Andersland and Ladanyi, *An Introduction to Frozen Ground Engineering*; Kondo and Haginoya, "Characteristic Heat Transfer Coefficients Near the Ground at Night During Strong Winds"; Groen, "Note on the Theory of Nocturnal Radiational Cooling of the Earth's Surface"; Saha, "Heat Balance of the Earth's Surface – Upward and Downward Transfer of Heat"; Arya, *Introduction to Micrometeorology*; Alkhaier, Schotting, and Su, "A Qualitative Description of Shallow Groundwater Effect on Surface Temperature of Bare Soil"; Alkhaier, Flerchinger, and Su, "The Thermodynamic Effect of Shallow Groundwater on Temperature and Energy Balance at Bare Land Surface, Heat Analysis and Thermodynamic Effects"; Alkhaier, Flerchinger, and Su, "Shallow Groundwater Effect on Land Surface Temperature and Surface Energy Balance Under Bare Soil Conditions: Modeling and Description"; Alkhaier, Su, and Flerchinger, "Reconnoitering the Effect of Shallow Groundwater on Land Surface Temperature and Surface Energy Balance Using MODIS and SEBS"; Alkhaier, "Shallow Groundwater Effect on Land Surface Temperature and Surface Energy Balance: Description, Modeling and Remote Sensing Application."

[19] Andersland and Ladanyi, *An Introduction to Frozen Ground Engineering*; Kondo and Haginoya, "Characteristic Heat Transfer Coefficients Near the Ground at Night During Strong Winds"; Groen, "Note on the Theory of Nocturnal Radiational Cooling of the Earth's Surface"; Arya, *Introduction to Micrometeorology*; Saha, "Heat Balance of the Earth's Surface – Upward and Downward Transfer of Heat."

[20] Christian Haselwimmer and Anupma Prakash, "Thermal Infrared Remote Sensing of Geothermal Systems," in *Thermal Infrared Remote Sensing: Sensors, Methods, Applications*, ed. Claudia Kuenzer and Stefan Dech, Remote Sensing and Digital Image Processing (Springer Netherlands, 2013).

[21] John H. Lienhard IV and John H. Lienhard V, *A Heat Transfer Textbook*, 4th ed. (Cambridge, MA, USA: Phlogiston Press, 2012).

[22] Alkhaier, Schotting, and Su, "A Qualitative Description of Shallow Groundwater Effect on Surface Temperature of Bare Soil"; Alkhaier, Flerchinger, and Su, "The Thermodynamic Effect of Shallow Groundwater on Temperature and Energy Balance at Bare Land Surface, Heat Analysis and Thermodynamic Effects"; Alkhaier, Flerchinger, and Su, "Shallow Groundwater Effect on Land Surface Temperature and Surface Energy Balance Under Bare Soil Conditions: Modeling and Description"; Alkhaier, Su, and Flerchinger, "Reconnoitering the Effect of Shallow Groundwater on Land Surface Temperature and Surface Energy Balance Using MODIS and SEBS"; Alkhaier, "Shallow Groundwater Effect on Land Surface Temperature and Surface Energy Balance: Description, Modeling and Remote Sensing Application."